Available online at www.sciencedirect.com

ScienceDirect

Procedia CIRP 43 (2016) 52 – 57

www.elsevier.com/locate/procedia

14th CIRP Conference on Computer Aided Tolerancing (CAT)

Tolerance Analysis By Polytopes: Application To Assembly Interferences Diagnosis

Doriane Gouyou*, Denis Teissandier, Vincent Delos

Univ. Bordeaux, I2M, UMR 5295, F-33400 Talence, France

* Corresponding author. Tel.: +33-5-4000-6220; fax: +33-5-4000-6964. *E-mail address: doriane.gouyou@u-bordeaux.fr*

Abstract

One way to perform tolerance analysis on over-constrained mechanical systems is to manipulate sets of constraints. During the 25 last years, several models (domains by Giordano et al., polytopes by Teissandier et al. or T-Maps by Davidson et al.), have been developed to control the assembly of parts without contact interferences. In general, if the intersection between sets of contact constraints is non empty, it is possible to perform an assembly made up of two parts without interference. Then, several works have been realized to qualify the clearance of the assembly. On the other hand, if the intersection is an empty set, it is not possible to perform the assembly between two parts without interference (i.e. without induced strains by the assembly process). This paper will focus on the diagnosis of such empty sets.
Operations on n-polytopes ($1 \leq n \leq 6$) can be used to predict if an assembly made up of two parts can be performed without interferences. When parts cannot be assembled, the objective of engineers is also to determine the corrections that should be applied to them in order to achieve an assembly. The main objective of this paper is to present a method to determine these corrections. A protocol to find the origins of the interferences and to investigate about the possible modifications to suppress the interference contact between the fabricated parts is described. Finally, a diagnosis is performed and can be used to correct real parts or in some cases to correct manufacturing processes. An example will illustrate the proposed method.

Peer-review under responsibility of the organizing committee of the 14th CIRP Conference on Computer Aided Tolerancing
Keywords: Tolerance analysis; over-constrained mechanisms; polytopes; intersection; contact interference; polytope distance

1. Introduction

Tolerance analysis consists of simulating the behaviour of a mechanical system, taking account of the geometric defects of its constituent parts. As some mechanisms produced industrially are strongly hyperstatic (i.e. over-constrained), those defects can lead to assembly interferences.

Different models using set of constraints have been developed to detect those interferences. This concept has been introduced by Fleming in 1987 [1]. In this way, all relative positions between two surfaces potentially in contact or the positions of a surface in a tolerance zone can be characterised. Several studies have been carried out using this principle: these include feasibility spaces [2], T-Maps [3], Domains [4] and [5], Polyhedra, and Polytopes [6] for example.

In this study, we use the polytope method to verify that parts assembly is possible and if interferences are detected, we propose a method to diagnose those interferences and correct the parts to insure the assembly.

This approach is unusual in that involves manipulating only finite and bounded sets of linear constraints [6], [7] and [8]. This represents a fundamental difference in formalising operations on sets of constraints, as required in tolerance analysis: Minkowski sum and intersection. The reason for this approach is to use the cumulative calculations of part defects based on Minkowski sums [9] and [10].

In addition, the method for calculating the polytope uses HV-description [11]. In this way, topological relations are retained between the vertices and facets of a polytope that correspond respectively to the relative extremal positions of two parts of a mechanism, and to the contact constraints. We shall return to this point later in the article.

In the first part of the article, the geometric variations of a clamp are defined in order to configure the polytope that can characterise it. We show how this polytope ensures that a clamp can be assembled.

Then, if assembly interferences are detected, we determine how to correct the parts or eventually the production

Peer-review under responsibility of the organizing committee of the 14th CIRP Conference on Computer Aided Tolerancing
doi:10.1016/j.procir.2016.02.019

processes.

Finally, we present our conclusions and prospects for future studies.

2. Characterisation of geometric variations in a clamp by a polytope

2.1. Modelling a clamp

A clamp-type joint is a rigid joint. It consists of a planar pair joint and several ball and cylinder pair joints held by pin / hole pairs distributed around a circle.

Fig. 1 shows a clamp between parts 1 and 2. It is made up of five pin / hole pairs, each of which is modelled by a ball and cylinder pair joint rather than a cylindrical pair type joint as the hole is short in length.

This type of architecture is highly hyperstatic, and is often used in aeronautics, space, nuclear physics, etc. Usually the parts are held in position by bolts, but these are not considered in this study and are not shown in Fig. 1.

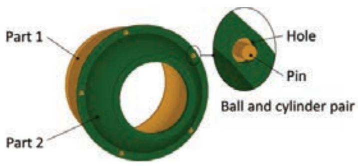

Fig. 1 – Clamp

The part to which the pins are fixed is part 1 and the part with the holes is part 2.

The aim of the study is to verify that clamp can be assembled. If interferences are detected, corrections of parts to insure the assembly are determined.

The following hypotheses are put forward:

- No deformable solids,
- No local strain in surfaces in contact,
- No form defect.

The real surfaces of the parts are modelled by substituted surfaces. Surfaces 1,1; 1,2; … ; 1,5 and 2,1; 2,2; … ; 2,5 are cylindrical and surfaces 1,6 and 2,6 are planar (see Fig. 2). In the nominal configuration defined in CAD, the axes of the cylindrical surfaces are parallel to the nominal axis of the clamp. In addition, they are equidistributed around a circle included in the plane and centred on the nominal axis of the clamp. The planar surfaces are coincident and normal to the clamp axis: they define the clamp plane.

2.2. Definition of geometric variables

Only location deviations and deviations in the diameters of the pins and holes are considered. These can potentially cause interferences in assembly for a given population of parts 1 and 2.

Let $R_0(O, \boldsymbol{x_0}, \boldsymbol{y_0}, \boldsymbol{z_0})$ be the reference system associated with the nominal geometry of the parts. Points $N_{0i}\left(i \in \{1,...,5\}\right)$ are the respective nominal positions of the pin 1,i / hole 2,i pairs in the clamp plane. The origin O of reference system R_0 is the centre of the circle Ce_0 with radius R_{th} passing through points $N_{0i}\left(i \in \{1,...,5\}\right)$. The axis $O\boldsymbol{x_0}$ passes through the point N_{01} (see Fig. 3).

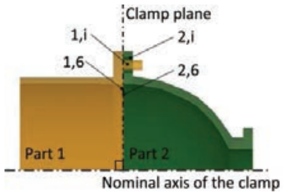

Fig. 2 – Parameters setting of substituted surfaces ($i \in [1,5]$)

Fig. 3a shows the nominal model of the clamp. This corresponds to the CAD model which is a specific occurrence when producing parts 1 and 2, such that all geometric variations inherent in the production and assembly processes are null. The centres of pins 1,i and holes 2,i coincide with their nominal locations $N_{0i}\left(i \in \{1,...,5\}\right)$. The diameters of pins 1,i and holes 2,i coincide with the nominal diameter D_n. Local clearances (c_i with $i \in \{1,...,5\}$) are null.

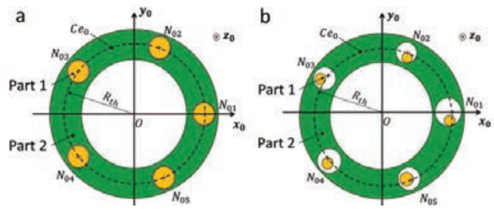

Fig. 3 – (a) Nominal geometry of parts; (b) Real geometry of parts

Fig. 3b shows the modelling of a real clamp. The geometric variations of parts 1 and 2 are modelled in the clamp plane. Between parts 1 and 2, only translations following axes $\boldsymbol{x_0}$ and $\boldsymbol{y_0}$, and rotation around axis $\boldsymbol{z_0}$ are considered.

2.3. Expression of polytope resulting from a clamp

In this part, we show how to express the polytope resulting from the clamp as a function of the variables used to configure the geometry of parts 1 and 2. The resulting polytope simulates the assembly of parts 1 and 2 and detects whether or not interferences are present.

Table 1 – Setting of clamp parameters ($i \in \{1,...,5\}$)

Nominal geometry (Fig. 3a)		Theoretical implantation radius of pins and holes	R_{th}
		Theoretical implantation angles of pins and holes	θ_{th_i}
		Nominal diameters of pins and holes	D_n
Real geometry (Fig. 3b)	Pins	Real diameters	$D_{1,i}$
		Location deviations along $\boldsymbol{x_0}$	$e_{N_{0i}-1,i/1,0_x}$
		Location deviations along $\boldsymbol{y_0}$	$e_{N_{0i}-1,i/1,0_y}$
	Holes	Real diameters	$D_{2,i}$
		Location deviations along $\boldsymbol{x_0}$	$e_{N_{0i}-2,i/2,0_x}$
		Location deviations along $\boldsymbol{y_0}$	$e_{N_{0i}-2,i/2,0_y}$

The parts simulated to calculate the resulting polytope show production defects. Those defects (location deviations and deviations in diameters of the pins and holes) come from measurements made on real parts. The names of the variables used to model these defects are given in Table 1.

Fig. 4 shows an illustration of the variables given in Table 1 for a pin 1,i / hole 2,i pair.

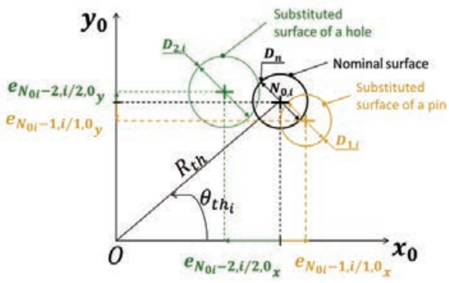

Fig. 4 – Parameters setting of geometrical deviations of pin 1,i / hole 2,i pair

Nominal geometry is defined by constant nominal and theoretical variables: they can be extracted directly from a CAD model (see Table 1).

Real geometry defines the production defects of parts 1 and 2 (see Table 1).

The specific feature of the polytope method is that contact constraints are calculated for a finite number of points [11]. In our example, we decided arbitrarily to calculate these constraints at six points (see Fig. 5).

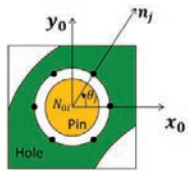

Fig. 5 – Contact constraints discretization

Local contact constraints between a pin 1,i and a hole 2,i at point N_{0i} are defined by the following relation:

$$\forall i \in \{1,...,5\}, \forall j \in \{1,...,6\}, \quad \boldsymbol{\varepsilon_{N_{0i}\text{-}1,i/2,i}}.\boldsymbol{n_j} \leq \frac{c_i}{2} \tag{1}$$

With:

- $\boldsymbol{\varepsilon_{N_{0i}\text{-}1,i/2,i}}$: vector of location deviations in N_{0i} of pin 1,i in relation with hole 2,i,
- c_i : local clearance of pin 1,i / hole 2,i pair with: $c_i = D_{2,i} - D_{1,i}$,

Contact constraints of each pin 1,i / hole 2,i pair are calculated at point O.

According to the small displacement field property [12]:

$$\boldsymbol{\varepsilon_{O\text{-}1,0/2,0}} = \boldsymbol{\varepsilon_{N_{0i}\text{-}1,0/2,0}} + \boldsymbol{ON_{0i}} \times \boldsymbol{\rho_{1,0/2,0}} \tag{2}$$

With :

- $\boldsymbol{\varepsilon_{N_{0i}\text{-}1,0/2,0}}$: vector of location deviations in N_{0i} of the nominal geometry of part 1 in relation to the nominal geometry of part 2.
- $\boldsymbol{\rho_{1,0/2,0}}$: rotation vector of the nominal geometry of part 1 in relation to the nominal geometry of part 2.

These two vectors characterise the relative small displacement between parts 1 and 2 at point O : these are the unknowns in the problem.

Let us express the vector $\vec{\varepsilon}_{N_{0i}-1,i/2,i}$ defined in (1) as a function of vector $\boldsymbol{\varepsilon_{N_{0i}\text{-}1,0/2,0}}$, of the parameters defining the nominal geometry and the manufactured geometry listed in Table 1.

Vector $\boldsymbol{\varepsilon_{N_{0i}\text{-}1,i/2,i}}$ can be expressed as a function of the manufacturing deviations in pin 1,i and hole 2,i (see Fig. 4). Then:

$$\forall i \in \{1,...,5\}, \ \boldsymbol{\varepsilon_{N_{Oi}\text{-}1,i/2,i}} = \boldsymbol{\varepsilon_{N_{Oi}\text{-}1,i/1,0}} + \boldsymbol{\varepsilon_{N_{Oi}\text{-}1,0/2,0}} - \boldsymbol{\varepsilon_{N_{Oi}\text{-}2,i/2,0}} \tag{3}$$

With :

- $\boldsymbol{\varepsilon_{N_{0i}\text{-}1,i/1,0}}$: vector of the location deviations from the centre of pin 1,i in relation to the nominal geometry of part 1, $\boldsymbol{\varepsilon_{N_{Oi}\text{-}1,i/1,0}} = e_{N_{Oi}\text{-}1,i/1,0_x}.\boldsymbol{x_0} + e_{N_{Oi}\text{-}1,i/1,0_y}.\boldsymbol{y_0}$ (see Table 1)
- $\boldsymbol{\varepsilon_{N_{0i}\text{-}2,i/2,0}}$: vector of the location deviations from the centre of pin 2,i in relation to the nominal geometry of part 2; $\boldsymbol{\varepsilon_{N_{Oi}\text{-}2,i/2,0}} = e_{N_{Oi}\text{-}2,i/2,0_x}.\boldsymbol{x_0} + e_{N_{Oi}\text{-}2,i/2,0_y}.\boldsymbol{y_0}$ (see Table 1)

Finally, the contact constraints between a pin 1,i and a hole 2,i at point N_{0i} can be written according to (1) and (3):

$$\forall i \in \{1,...,5\}, \forall j \in \{1,...,6\},$$
$$(\boldsymbol{\varepsilon_{N_{0i}\text{-}1,i/1,0}} + \boldsymbol{\varepsilon_{N_{0i}\text{-}1,0/2,0}} - \boldsymbol{\varepsilon_{N_{0i}\text{-}2,i/2,0}}).\boldsymbol{n_j} \leq \frac{c_i}{2} \tag{4}$$

According to (2), we can express $\boldsymbol{\varepsilon_{N_{0i}\text{-}1,0/2,0}}$ as a function of $\boldsymbol{\varepsilon_{O\text{-}1,0/2,0}}$ and $\boldsymbol{\rho_{1,0/2,0}}$ (unknowns in the problem).

We can then deduce the contact constraints for any pin 1,i / hole 2,i pair expressed at point O as a function of the manufacturing defects of parts 1 and 2:

$$\begin{aligned} &\forall i \in \{1,...,5\}, \forall j \in \{1,...,6\}, \\ &\left(e_{N_{Oi}\text{-}1,i/1,0_x} + \varepsilon_{O\text{-}1,0/2,0_x} - e_{N_{Oi}\text{-}2,i/2,0_x}\right).\cos(\theta_j) \\ &+\left(e_{N_{Oi}\text{-}1,i/1,0_y} + \varepsilon_{O\text{-}1,0/2,0_y} - e_{N_{Oi}\text{-}2,i/2,0_y}\right).\sin(\theta_j) \\ &+\rho_{1,0/2,0_z}.R_{th}.\sin(\theta_j - \theta_{th_i}) \leq \frac{c_i}{2} \end{aligned} \tag{5}$$

When considering the base ($\boldsymbol{x_0}, \boldsymbol{y_0}, \boldsymbol{z_0}$):

$$\boldsymbol{\varepsilon_{O\text{-}1,0/2,0}} \begin{pmatrix} \varepsilon_{O\text{-}1,0/2,0_x} \\ \varepsilon_{O\text{-}1,0/2,0_y} \\ 0 \end{pmatrix}, \boldsymbol{N_{0i}O} \begin{pmatrix} -R_{th}.\cos\left(\theta_{th_i}\right) \\ -R_{th}.\sin\left(\theta_{th_i}\right) \\ 0 \end{pmatrix} \text{ and } \boldsymbol{\rho_{1,0/2,0}} \begin{pmatrix} 0 \\ 0 \\ \rho_{1,0/2,0_z} \end{pmatrix}$$

The operand polytope P_i , which characterises the contact constraints of the pin 1,i / hole 2,i pair results from the intersection of the 6 half-spaces (5). Relation (5) is the H-description of an operand polytope [11].

We put forward the following hypothesis:

$$\frac{c_i}{2} \geq 0 \tag{6}$$

Hypothesis of equation (6) implies that any operand polytope is a 3-dimension polytope.

We write as $\overline{H}^-_{i,j}$ the 3-dimension half-space of the contact constraint derived from discretization point j of the pin 1,i / hole 2,i pair; after (5) we have equation (7) :

$$\forall i \in \{1,...,5\}, \forall j \in \{1,...,6\},$$
$$\overline{H}^-_{i,j} = a_{j1}.x_1 + a_{j2}.x_2 + a_{j3}.x_3 \leq b_{ij} \tag{7}$$

With:

- $a_{j1} = R_{th}.\sin\left(\theta_j - \theta_{th_i}\right)$ and $x_1 = \rho_{1,0/2,0_z}$
- $a_{j2} = \cos\left(\theta_j\right)$ and $x_2 = \varepsilon_{O-1,0/2,0_x}$
- $a_{j3} = \sin\left(\theta_j\right)$ and $x_3 = \varepsilon_{O-1,0/2,0_y}$
- $b_{i,j} = \frac{c_i}{2} + \left(e_{N_{0i}-2,i/2,0_x} - e_{N_{0i}-1,i/1,0_x}\right).\cos\left(\theta_j\right) + \left(e_{N_{0i}-2,i/2,0_y} - e_{N_{0i}-1,i/1,0_y}\right).\sin\left(\theta_j\right)$

Variables xi (i.e. $\rho_{1,0/2,0_z}$, $\varepsilon_{O-1,0/2,0_x}$ and $\varepsilon_{O-1,0/2,0_y}$) are the unknowns in the problem. Finally, the operand polytope P_i , which characterises the contact constraints of the pin 1,i / hole 2,i pair results from the intersection of the half-spaces $\overline{H}^-_{i,j}$.

$$\forall i \in \{1,...,5\}, \quad P_i = \bigcap_{j=1}^{6} \overline{H}^-_{i,j} \tag{8}$$

Fig. 6 shows the operand polytope P_i calculated at O .

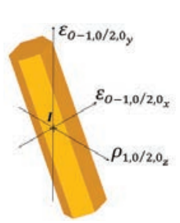

Fig. 6 - Operand polytope at point O

The polytope resulting from the clamp, P_R , is obtained by calculating the intersection of the five operand polytopes P_i at point O (see Fig. 7a).

$$P_R = \bigcap_{i=1}^{5} P_i = \bigcap_{i=1}^{5} \left(\bigcap_{j=1}^{6} \overline{H}^-_{i,j} \right) \tag{9}$$

Equation (9) is the H-description of the resulting polytope [11].

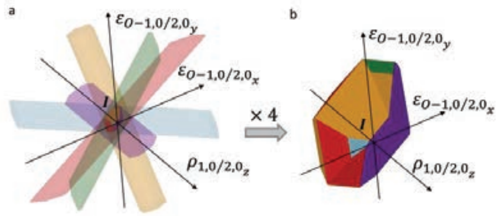

Fig. 7 – (a) Operand polytopes intersection; (b) Resultant polytope

The parts can be assembled without interference if all the pin 1,i / hole 2,i local clearances are strictly positive for some relative positions in part 1 and part 2 (see Fig. 8a).

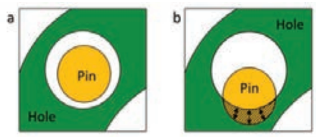

Fig. 8 – (a) Positive local clearances; (b) Negative local clearances

Mathematically, this translates as the condition that the resulting polytope defined by (9) is non-empty. The resulting polytope then describes all possible displacements between parts 1 and 2. Each displacement is defined as a translation in the ($\boldsymbol{x_0}, \boldsymbol{y_0}$) plane and a rotation around axis $\boldsymbol{z_0}$, see Fig. 7b.

If some local clearances are negative, whatever the relative positions between parts 1 and 2, part 1 cannot be assembled with part 2 without interferences (see Fig. 8b).

Mathematically, this translates as a resulting polytope equal to an empty intersection.

3. Assembly interferences diagnosis

In this part, we show how to diagnosis interferences in assembly of parts 1 and 2. The method used enables to identify pin 1,i / hole 2,i pairs responsible of those interferences and more precisely the contact area generating those interferences (i.e. identification of discretization points).

We put forward the following hypothesis: polytope P_R resulting from the clamp can always be seen as the intersection of two non-empty subsets.

Let us consider a clamp with five pin 1,i / hole 2,i pairs of which the resulting polytope is empty. The first four pin 1,i /hole 2,i can be assembled without interferences.

$$P_R = P_{1234} \cap P_5 = \varnothing$$
$$\text{with } P_{1234} = \bigcap_{i=1}^{4}\left(\bigcap_{j=1}^{6} \overline{H}_{i,j}^{-}\right) \neq \varnothing \text{ and } P_5 = \bigcap_{j=1}^{6} \overline{H}_{5,j}^{-} \neq \varnothing \quad (10)$$

Fig. 9a shows polytopes P_{1234} and P_5.

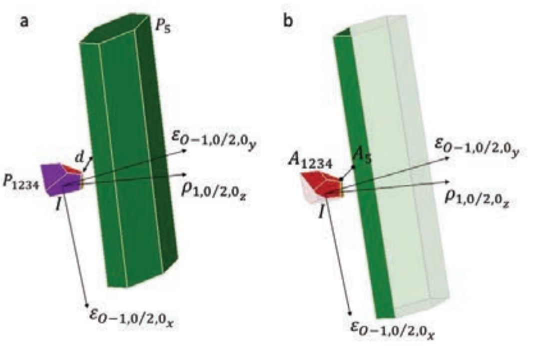

Fig. 9 – (a) Polytopes P_{1234} and P_5; (b) Dots A_{1234} and A_5

Whatever the relative positions between parts 1 and 2, after assembly of the first four pin 1,i / hole 2,i ($i \in [1,4]$), the pin 1,5 cannot be assembled with the hole 2,5 without interferences. The aim is to determine the minimum corrections of parts to suppress those interferences (i.e. to guaranty that the intersection of polytopes P_{1234} and P_5 is non-empty).

Fabrication deviations of parts 1 and 2 (location and diameter deviations of pins and holes) only affect the values of second member b_{ij} of half-spaces $\overline{H}_{i,j}^{-}$: see (7). A modification of parameters b_{ij} causes a translation of respective half-spaces $\overline{H}_{i,j}^{-}$. Let us find the minimum translations of half-spaces $\overline{H}_{i,j}^{-}$ which guaranty a non-empty intersection of polytopes P_{1234} and P_5 . Those translations depend on the minimum distance d between polytopes P_{1234} and P_5 (see Fig. 9a). The distance d can be determined using a quadratic optimisation. It can be calculated with the program Polytope Distance of CGAL [13].

Let be V_{1234} and V_5 the sets of respective vertices of polytopes P_{1234} and P_5. Those sets are the V-descriptions of polytopes P_{1234} and P_5.

$V_{1234} = \{v_i \mid i \in \{1,...,r\}\}$ and $V_5 = \{v_i' \mid i \in \{1,...,s\}\}$ with r the number of P_{1234} vertices and s the number of P_5 vertices.

Let be $x^* = \{x_i^* \mid i \in \{1,...,n\}\}$ an optimal solution to:

$$\begin{aligned} &\textit{minimize} && x^T C^T C x \\ &\textit{subject to} && \sum_{i=1}^{r} x_i = 1 \\ & && \sum_{i=r+1}^{n} x_i = 1 \\ & && x \geq 0 \end{aligned}$$

with $n = r + s$ and $C = \{v_1, \ldots, v_r, -v_1', \ldots, -v_s'\}$.

The support sets are determined by the positive x_i^*, namely

$v = \{v_i \in V_{1234} \mid x_i^* > 0\}$,

$v' = \{v_i' \in V_5 \mid x_{r+i}^* > 0\}$.

The realizing points are convex combinations of the given points i.e. in the base $\left(\rho_{1,0/2,0_z}, \varepsilon_{O-1,0/2,0_x}, \varepsilon_{O-1,0/2,0_y}\right)$:

$$A_{1234} = \sum_{i=1}^{r} x_i^* . v_i = \begin{pmatrix} 0,0044 \\ -0,0015 \\ -0,0008 \end{pmatrix}$$

$$A_5 = \sum_{i=1}^{s} x_{i+r}^* . v_i' = \begin{pmatrix} 0,0020 \\ -0,0043 \\ 0,0042 \end{pmatrix}$$

Points A_{1234} and A_5 are shown in Fig. 9b.

Those points are located on the boundaries of polytopes P_{1234} and P_5. In R^3, each point can be on a vertex, an edge or a facet.

The generator of each resulting polytope facet is a boundary of one half-space among the 5×6 half-spaces $\overline{H}_{i,j}^{-}$ of operands, see (9).

The method used here to calculate polytopes is based on a truncation algorithm developed in the Politopix software toolbox [14]; it is able to identify the generator of each resultant polytope facet obtained from intersection operations. The truncation algorithm is based on the intersection of the half-spaces of a polytope (i.e. its H-description) [6], [11], [14].

This algorithm is able to determine the V-description of a polytope from its H-description (i.e; the double description).

Then, it is possible to determine which half-spaces of operands generates each vertex, edge or facet of polytope P_{1234}. Each half-space corresponds with a discretization point, the areas of pin 1,i / hole 2,i pairs generating each vertex, edge or facet of polytopes P_{1234} and P_5 can be identified.

The point A_{1234} is generated by the intersection of three facets of P_{1234} (see Fig. 9b). Those facets are from:

- Discretization point 2 of pin 1,1 / hole 2,1
- Discretization point 3 of pin 1,3 / hole 2,3
- Discretization point 4 of pin 1,3 / hole 2,3

The point A_5 is located on an edge of P_5. That edge is generated by the intersection of two facets (see Fig. 9b). Those facets are from:

- Discretization point 5 of pin 1,5 / hole 2,5
- Discretization point 6 of pin 1,5 / hole 2,5

Fig. 10 shows the minimal interference in assembly of pin 1,5 / hole 2,5 pair when the four pin 1,i / hole 2,i pairs ($i \in \{1,...,4\}$) are assembled.

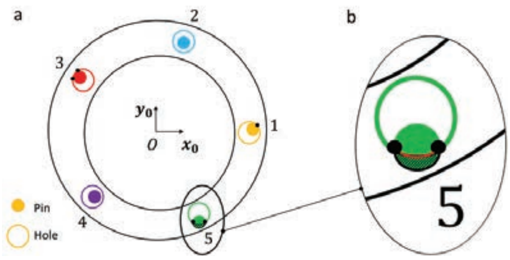

Fig. 10 – Assembly interferences

Elements of vector $\boldsymbol{A_5A_{1234}}$ indicate the direction and amplitude of modifications that have to be made on part 1 and/or part 2. That vector characterises the minimal translation of half-spaces $\overline{H}^{-}_{i,j}$ to obtain a non-empty intersection.

The suppression of interferences in assembly of parts 1 and 2 consists in setting the norm of vector $\boldsymbol{A_5A_{1234}}$ to zero.

Theoretically, this can be realised by changing some pin and/or hole diameters, and/or by changing the locations of pin and/or hole centres. In practice, the simplest operation consists in extending hole diameters.

Let us choose to only translate facets of polytope P_5.

Point A_5 indicates where hole 2,5 should be corrected: between discretization points 5 and 6 (see Fig. 10b). This information is not used in this example as the entire hole is extended.

Elements $\varepsilon_{O-1,0/2,0_x}$ and $\varepsilon_{O-1,0/2,0_y}$ of vector $\boldsymbol{A_5A_{1234}}$ are used to determine the value $d_{2,5}$ corresponding to augmentation of diameter $D_{2,5}$ to suppress interferences in assembly.

$$d_{2,5} = 2.\sqrt{{\varepsilon_{O-1,0/2,0_x}}^2 + {\varepsilon_{O-1,0/2,0_y}}^2} \approx 12\mu m \tag{11}$$

With this approach, pin 1,i / hole 2,i pairs and discretization points responsible for interferences can be identified. Location, amplitude and direction of corrections can be determined. This method can be used to correct non-conform parts or manufacturing processes.

4. Conclusion, overview and future prospects

In this study, we have shown how to model a clamp using the polytope method. With this approach the real assembly of two parts can be simulated based on their manufacturing defect. If the polytope resulting from the clamp is non-empty, the parts can be assembled without interference. If the polytope resulting from the joint is totally empty, the parts cannot be assembled without interference and those interferences can be diagnosed.

Traceability between the H-description of the polytopes and the contact constraints enables us to determine which pin 1,i / hole 2,i pair(s) and which discretization point(s) is/are causing interferences in the assembly. Then, it is possible to find out precisely what changes have to be made directly to the parts or to the manufacturing processes.

All simulations were performed using the PolitoCAT and Politopix software tools, available on Open source [14]. Although the study described in this article was carried out in a 3D affine space, this method can be transposed to affine spaces with larger dimensions using PolitoCAT and Politopix.

In future studies, we intend to introduce strains into the parts in the polytope calculation method. This will enable us to simulate assemblies that are more representative of the real assembly produced in the workshop in the case of flexible parts.

5. Références

[1] A. D. Fleming, « Geometric relationships between toleranced features », *Artif. Intell.*, vol. 37, n° 1‑3, p. 403‑412, 1988.

[2] J. U. Turner, « A Feasability Space Appoach for Automated Tolerancing », *J. Eng. Ind.*, vol. 115, p. 341‑346, 1993.

[3] J. K. Davidson, A. Mujezinovic, et J. J. Shah, « A new mathematical model for geometric tolerances as applied to round faces », *ASME Trans. J. Mech. Des.*, vol. 124, p. 609‑622, 2002.

[4] M. Giordano, D. Duret, S. Tichadou, et R. Arrieux, « Clearance space in volumic dimensioning », *Ann. CIRP*, vol. 41, n° 1, p. 565–568, 1992.

[5] M. Mansuy, M. Giordano, et J. K. Davidson, « Comparison of Two Similar Mathematical Models for Tolerance Analysis: T-Map and Deviation Domain », *J. Mech. Des.*, vol. 135, n° 101008‑1/101008‑7, 2013.

[6] D. Teissandier, V. Delos, et Y. Couétard, « Operations on polytopes: application to tolerance analysis », in *Global Consistency of Tolerances*, Enschede (Netherlands), 1999, p. 425‑433.

[7] L. Homri, D. Teissandier, et A. Ballu, « Tolerancing analysis by operations on polytopes », in *Design and Modeling of Mechanical Systems*, Djerba (Tunisie), 2013, p. 597‑604.

[8] L. Homri, D. Teissandier, et A. Ballu, « Tolerance analysis by polytopes: Taking into account degrees of freedom with cap half-spaces », *Comput.-Aided Des.*, vol. 62, p. 112‑130, mai 2015.

[9] Y. Wu, J. J. Shah, et J. K. Davidson, « Improvements to algorithms for computing the Minkowski sum of 3-polytopes », *Comput.-Aided Des.*, vol. 35, n° 13, p. 1181‑1192, 2003.

[10] D. Teissandier et V. Delos, « Algorithm to calculate the Minkowski sums of 3-polytopes based on normal fans », *Comput.-Aided Des.*, vol. 43, p. 1567‑1576, 2011.

[11] G. Ziegler, *Lectures on polytopes*. ISBN 0-387-94365-X, Springer Verlag, 1995.

[12] A. Clément et P. Bourdet, « A study of optimal-criteria identification based on the small-displacement screw model », *Ann. CIRP*, vol. 37, n° 1, 1988.

[13] S. Schonherr, « Quadratic Programming in Geometric Optimization: Theory, Implementation and Applications », 2002.

[14] V. Delos et D. Teissandier, *PolitoCAT and Politopix*, *http://i2m.u-bordeaux.fr/politopix.html*. 2015.